

Synthesis of new microporous layered organic–inorganic hybrid nanocomposites by alkoxylation of a crystalline layered silicate, ilerite

Ryo Ishii,* Takuji Ikeda, Tetsuji Itoh, Takeo Ebina, Toshiro Yokoyama, Takaaki Hanaoka and Fujio Mizukami

Received 14th July 2006, Accepted 17th August 2006

First published as an Advance Article on the web 31st August 2006

DOI: 10.1039/b610088k

We have developed microporous organic–inorganic hybrid nanocomposites by alkoxylation of 4,4'-biphenyl-bridged alkoxy silane compounds, which contain triethoxysilyl, methyldiethoxysilyl, and dimethylethoxysilyl groups at each end of the 4,4'-biphenylene unit $((\text{CH}_3)_n(\text{C}_2\text{H}_5\text{O})_{3-n}\text{-Si-C}_{12}\text{H}_8\text{-Si-(OC}_2\text{H}_5)_{3-n}(\text{CH}_3)_n, n = 0, 1, \text{ or } 2$, abbreviated as BESB(0), BESB(2), or BESB(4), respectively, where the number in parentheses indicates the number of methyl groups in these molecules), in the interlayer of a crystalline layered silicate, ilerite. XRD, ^{29}Si solid-state NMR and fluorescence spectroscopy revealed the immobilization and bridging formation of the BESB molecules between the silicate layers by condensation, not only with H-ilerite, but also with the BESB molecules. The interlayer structures exhibited different molecular arrangements. BESB(0) and BESB(4) molecules are present as a monolayer arrangement in which BESB(0) molecules form the oligomeric species caused by close stacking like a dimer. BESB(2) molecules form mainly bilayer-like aggregates in the interlayer. The structural differences are caused by the different reactivities of the BESB molecules, which control their polymerization in the interlayer. The resultant BESB(0)- and BESB(2)-ilerite had high microporosity with BET surface areas (508 and $578 \text{ m}^2 \text{ g}^{-1}$ for BESB(0)- and BESB(2)-ilerite, respectively). The micropores showed higher toluene adsorptivity than several other porous silica materials due to the successful surface modification. Consequently, this approach provides a new method for constructing novel microporous nanocomposites, the key to improved selectivity and activity in separation and catalytic applications.

1. Introduction

Construction of novel organic–inorganic hybrid nanocomposites using crystalline layered silicates such as kanemite, ilerite, magadiite and other layered silicates has attracted much attention in inorganic materials fields. Typical nanocomposites are organically modified layered silicates that have been synthesized by surface modification using silylation with organochlorosilane compounds.^{1–9} The resultant nanocomposites possess a hydrophobic liquid in the interlayer due to intercalated alkyl groups, and have potential applications as adsorbents or fillers in polymer composites. On the other hand, the nanocomposites have no vacant spaces (micropores) in the interlayer due to the bulky, flexible alkyl groups. This reduces selectivity for the accommodation of specific guest molecules in the interlayer, limiting their application as adsorbents or functional materials.

Recently, many efforts have been devoted to the design and construction of an open framework in the interlayer spaces of crystalline layered silicates. The basic strategy is to create a bridging formation between the silicate layers by utilizing periodic and reactive silanol groups on both surfaces in the

interlayer. Some research groups have successfully reported the formation of a three-dimensional open framework structure like zeolites by the condensation of silanols on both sides of the interlayer.^{10–13} Alternatively, Kuroda's group has demonstrated an indirect bridging formation by silylation with alkoxychlorosilanes on the layered silicates.^{14,15} The periodic silylation on the surface and the subsequent connection between the layers also form an open framework in the interlayer space. In addition, they have synthesized organically modified kanemite by periodic silylation with monochloro-, dichloro-, and alkyltrichlorosilanes.¹⁶ Some of the products exhibited microporosity in their interlayer because the organic moieties of the alkylchlorosilanes play the role of 'pillars' to preserve the interlayer space. Their work suggests that alkylsilylation focused on the periodic silanols has the potential to construct organic–inorganic nanocomposites with an open framework structure.

We have also synthesized organic–inorganic nanocomposites by creating a bridging formation between the silicate layers of ilerite through alkoxylation with 4,4'-bis(triethoxysilyl)biphenyl (BESB).¹⁷ BESB is one of the organic-bridging alkoxy silane compounds $((\text{R}_1\text{O})_3\text{-Si-R}_2\text{-Si-(OR}_1)_3; \text{R}_1 = \text{CH}_3 \text{ or } \text{C}_2\text{H}_5, \text{R}_2 = \text{-CH}_2\text{-}, \text{-C}_2\text{H}_2\text{-}, \text{-C}_6\text{H}_4\text{-}, \text{-C}_{12}\text{H}_8\text{-}, \text{ etc.})$ that have been extensively studied in the development of novel silica hybrid materials.^{18–22} The compound has reactive ethoxysilyl groups at each end of the biphenylene unit, leading to condensation with the silanol groups. The layered

Research Center for Compact Chemical Process, National Institute for Advanced Industrial and Science Technology (AIST), Nigatake 4-2-1, Miyagino, Sendai 983-8551, Japan. E-mail: ryo-ishii@aist.go.jp; Fax: +81 22 237 7027.; Tel: +81 22 237 3092

silicic acid of ilerite provides periodic and reactive silanol groups on the interlayer surface, which function as host compounds for the biphenylene-bridging alkoxy silane. Intercalation in the layered silicic acid caused anisotropic condensation with the silanols on both sides of the interlayer, producing a bridging formation of biphenylene moieties between the layers. The intercalation compound showed a layered structure of silicic layers and biphenylene units that play the role of pillars, retaining the interlayer space due to its rigidity. As a result, this material can be expected to be a novel microporous organic-inorganic nanocomposite that enables us to control the porosity and surface properties utilizing alkoxy silane compounds with various organic spacers.

Our previous report revealed that the bridging formation of the BESB molecules is accompanied by polymerization with each other, due to the excess number of ethoxy groups at each end of the biphenylene unit.¹⁷ It suggests that the control of the number of ethoxy groups provides an opportunity to produce various bridging formations such as mono- or multi-bridges, yielding various open framework structures. On the other hand, the mechanical stability of the pillars would be changed with the variations of the bridging formations, inducing the deterioration of certain open framework structures. Thus, alkoxy silylation using not only trifunctional, but also mono- and difunctional organic-bridging alkoxy silanes is a vital issue for the construction of this layered nanocomposite. In this study, we have investigated the bridging formation with three kinds of alkylalkoxy silane compound containing triethoxysilyl, methyldiethoxysilyl, and dimethylethoxysilyl groups at each end of the 4,4'-biphenylene unit $((\text{CH}_3)_n(\text{C}_2\text{H}_5\text{O})_{3-n}\text{-Si-C}_{12}\text{H}_8\text{-Si-(OC}_2\text{H}_5)_3\text{-}_n(\text{CH}_3)_n$, $n = 0, 1$ or 2 , abbreviated as BESB(0), BESB(2), or BESB(4), respectively, where the number in parentheses indicates the number of methyl groups in these molecules), for the first time. In the first part of this study, structural analyses of the resultant products were conducted in order to deduce the molecular arrangements of the biphenylene units in the interlayer. The porosity and adsorptivity of the products were then evaluated in order to determine their surface properties. Finally, we fabricated models of their open framework structures in the interlayer.

2. Experimental

Materials

Silica (Wako gel Q-63, Wako Pure Chemical Industries, Japan, reagent grade) was used for the synthesis of ilerite. Magnesium, *p*-nitroaniline (*p*NA) and 4,4'-dibromobiphenyl (Wako Pure Chemical Industries, Japan, reagent grade) were used as received. Tetraethylorthosilicate (TEOS, Wako Pure Chemical Industries, reagent grade), methyltriethoxysilane (Tokyo Kasei Kogyo Co., Ltd., Japan, reagent grade), and dimethyldiethoxysilane (Shin-Etsu Chemical Co., Ltd., Japan, reagent grade) were distilled from calcium hydride before use. Tetrahydrofuran, ethanol and *n*-hexane (Wako Pure Chemical Industries, dehydrated) were used without further purification.

Synthesis of ilerite and the corresponding silicic acid

Ilerite was prepared from a suspension containing 2 g of silica in 4 cm³ of 4 mol dm⁻³ NaOH aqueous solution at 378 K for 216 h, as described by Kosuge and Tsunashima.²³ Then, the silicic acid of ilerite (H-ilerite) was obtained by adding 70 cm³ of 0.1 mol dm⁻³ hydrochloric acid aqueous solution dropwise at a rate of 0.7×10^{-2} cm³ min⁻¹ to the synthesized ilerite. The acid treatment was repeated twice. The white product was washed with distilled water until Cl⁻ ions were no longer detected in the filtrate. H-Ilerite was then dried at 323 K overnight.

Synthesis of BESB(0), BESB(2), and BESB(4)

BESB(0) was synthesized according to the method reported by Shea *et al.*¹⁸ A solution of 4,4'-dibromobiphenyl (10 g) in THF (75 cm³) and TEOS (50 cm³) was added to magnesium turnings (3 g), and the mixture was refluxed at 348 K for 5 days. The mixture was then cooled to room temperature. After cooling, THF was removed *in vacuo* from the mixture and *n*-hexane (20 cm³) was newly added. The mixture was filtered under argon to remove precipitates in the mixture, after which *n*-hexane and the remaining TEOS were distilled off *in vacuo*. The resultant brown oil was distilled under *ca.* 0.3 mmHg at 508–518 K to give a clear oil (2.5 g, 16%). BESB(2) and BESB(4) were synthesized according to the same method using methyltriethoxysilane and diethoxydimethylsilane for BESB(2) and BESB(4), respectively, as a silicon source. Distillations were conducted under *ca.* 0.3 mmHg at 463–473 K and at 453–463 K for BESB(2) and BESB(4), respectively. They were obtained as colorless oils (BESB(2): 2.9 g, 22%; BESB(4): 3.1 g, 27%). NMR data of the compounds are as follows: BESB(0): δ_{H} (500 MHz; CDCl₃; Me₄Si) 7.77–7.62 (8 H, dd, C₆H₄), 3.90 (12 H, q, OCH₂CH₃), 1.27 (18 H, t, OCH₂CH₃); δ_{C} (126 MHz; CDCl₃; Me₄Si), 142.7 (C₆H₄, C), 135.3 (C₆H₄, CH), 129.9 (C₆H₄, C), 126.6 (C₆H₄, CH), 58.78 (OCH₂CH₃), 18.27 (OCH₂CH₃); BESB(2): δ_{H} (500 MHz; CDCl₃; Me₄Si), 7.73–7.62 (dd, 8 H, C₁₂H₈), 3.85 (q, 8 H, OCH₂CH₃), 1.26 (t, 12 H, OCH₂CH₃), 0.39 (s, 6 H, SiMe); δ_{C} (126 MHz; CDCl₃; Me₄Si), 142.5 (C₆H₄, C), 134.6 (C₆H₄, CH), 133.7 (C₆H₄, C), 126.6 (C₆H₄, CH), 58.58 (OCH₂CH₃), 18.38 (OCH₂CH₃), -4.09 (SiMe); BESB(4): δ_{H} (500 MHz; CDCl₃; Me₄Si), 7.67–7.63 (dd, 8 H, C₁₂H₈), 3.71 (q, 4 H, OCH₂CH₃), 1.21 (t, 6 H, OCH₂CH₃), 0.42 (s, 12 H, SiMe); δ_{C} (126 MHz; CDCl₃; Me₄Si), 142.1 (C₆H₄, C), 136.9 (C₆H₄, C), 134.0 (C₆H₄, CH), 126.6 (C₆H₄, CH), 58.73 (OCH₂CH₃), 18.47 (OCH₂CH₃), -1.66 (SiMe₂).

Condensation of BESB molecules in H-ilerite

H-Ilerite (0.2 g) was mixed with 1.2 cm³ of *n*-hexylamine and placed in a sealed Teflon tube for 2 days at room temperature. The H-ilerite and *n*-hexylamine mixture was stirred with BESB(0) (0.5 cm³) and *n*-hexane (10 cm³) for 7 days at room temperature. A white compound was separated from the suspension by centrifugation. The compound was then air-dried for 5 days at room temperature. After drying, the compound was suspended in 20 cm³ of 1 mol dm⁻³ HCl ethanol solution for 5 days at room temperature for the elution

of *n*-hexylamine. The final product (BESB(0)-ilerite) was separated and air-dried at 323 K overnight. The same procedure was conducted for the reaction of BESB(2) with the *n*-hexane and H-ilerite mixture. The final product is abbreviated as BESB(2)-ilerite.

The procedure with BESB(4) followed the same steps as with the BESB(0)-ilerite until the air-drying of the mixture of BESB(4), *n*-hexylamine, and H-ilerite for 5 days at room temperature. The HCl ethanol treatment after the drying led to the collapse of the interlayer space due to insufficient siloxane formation between BESB(4) and H-ilerite. Alternatively, the product was irradiated with microwaves for 30 min in an NE-M310 microwave oven (Matsushita Electric Industrial Co., Ltd., Japan, 500 W). The compound was then suspended in 23 cm³ of 1 N HCl aqueous solution for 5 days. After centrifugation, the product was stirred in ethanol at 343 K for 5 h. These steps were effective for the retention of the interlayer space. The final product (BESB(4)-ilerite) was air-dried at 323 K overnight.

Preparation of reference samples

As references, 4,4'-biphenyl-bridged polysilsesquioxane (polymerized BESB(0)) and cetyltrimethylammonium (CTA)-intercalated ilerite were prepared. BESB(0) (2 cm³) and *n*-hexylamine (2.3 cm³) were mixed and stirred for a day. After stirring, distilled water (1 cm³) was added dropwise. The solution immediately became a transparent gel. The gel was washed with ethanol and dried at 423 K overnight. A transparent solid was obtained (polymerized BESB(0), Brunauer–Emmett–Teller (BET) surface area = 2 m² g⁻¹). Ilerite (0.2 g) was stirred in CTA chloride solution (0.3 mol dm⁻³) at 423 K overnight. The product was centrifuged and washed with ethanol. A white product was obtained (CTA-ilerite).

Measurement of adsorption of *p*NA into BESB-ilerite's

BESB(0)-, BESB(2)-, and BESB(4)-ilerite (0.05 g) were degassed at 423 K below 10⁻³ mmHg for 2 h. After drying, they were stirred for 2 days in saturated *p*NA ethanol solution, the concentration of which was *ca.* 0.4 mol dm⁻³. The *p*NA-adsorbed BESB(0)-, BESB(2)-, and BESB(4)-ilerite were centrifuged from the solutions and then dried at 423 K overnight.

Characterization

Silicon contents of the samples were determined using an SPS7800 inductively coupled plasma (ICP) spectrometer (SEIKO Co., Japan) after melting in a mixture of H₃BO₃ and Na₂CO₃ (sample : Na₂CO₃ : H₃BO₃ = 1 : 5 : 1) and subsequently dissolved in a 5 mol dm⁻³ HCl solution. Total carbon (TC) and total nitrogen (TN) contents of the products were measured by gas chromatography with a SUMIGRAPH NCH-21 analyzer (Sumika Analysis Service Co., Ltd., Japan).

Powder X-ray diffraction (XRD) data were measured using an M21X diffractometer (MAC Science Co., Ltd, Japan) with curved graphite monochromator (Cu K_α radiation) operated at 45 kV and 250 mA. DTA-TG curves were collected on a Thermo plus TG8120 thermal analyzer (Rigaku Co., Ltd,

Japan) at a heating rate of 10 K min⁻¹. ²⁹Si solid-state MAS-NMR experiments were performed on a Bruker AVANCE 400 WB spectrometer operated at 79.495 MHz with a 7 kHz spinning frequency using a 7 mm MAS probe. ²⁹Si DDMAS NMR spectra were obtained with 30° pulses of 1.6 μs and 30 s cycle delay time. A total of 1024 scans were accumulated for each sample. UV-vis diffuse reflectance spectra for the products were obtained on a UV-3100PC spectrometer (Shimadzu Co., Ltd. Japan) coupled with an integrating sphere unit (MPC-3100, Shimadzu Co., Ltd. Japan) over the range of 200 to 400 nm after the compounds were mixed with barium sulfate powder and molded into pellet form. Fluorescence emission spectra were collected by an F-4500 fluorescence spectrometer (Hitachi Co., Ltd, Japan) over the range of 280 to 500 nm with excitation wavelength of 280 nm. Nitrogen adsorption and desorption measurements at 77 K were carried out on a Belsorp-28SA (Japan BEL Co. Ltd., Japan) for samples degassed at 423 K below 10⁻³ mmHg for 4 h. Toluene adsorption isotherms at 298 K were collected by a Belsorp-18 (Japan BEL Co. Ltd.) for samples degassed at 423 K below 10⁻³ mmHg for 6 h.

3. Results and discussion

3-1. Intercalation and alkoxylation with BESB in the interlayer of H-ilerite

XRD patterns of BESB(0)-, BESB(2)-, and BESB(4)-ilerite are presented in Fig. 1. These basal spacings are observed at $2\theta = 4.56, 3.29,$ and 5.34° for BESB(0)-, BESB(2)-, and BESB(4)-ilerite, respectively. The basal spacings shift to the lower side of 2θ than that of H-ilerite, indicating the intercalation of the biphenylene units. The corresponding *d*-values are 1.94, 2.68, and 1.65 nm for BESB(0)-, BESB(2)-, and BESB(4)-ilerite, respectively. The gallery height, which is

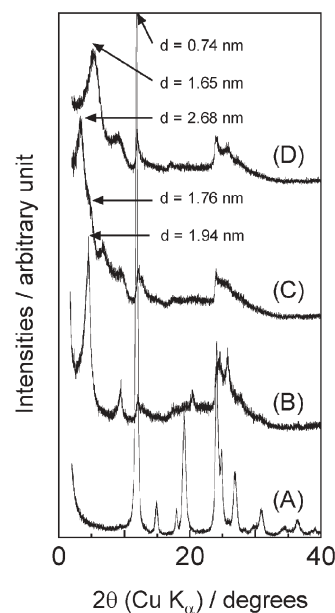


Fig. 1 XRD patterns of H-ilerite and biphenylene-bridged ilerites: (A) H-ilerite, (B) BESB(0)-ilerite, (C) BESB(2)-ilerite, and (D) BESB(4)-ilerite.

derived by subtracting the layer thickness (0.74 nm) of H-ilerite from the d -value, is calculated as 1.20 nm for BESB(0)-ilerite. It corresponds to the molecular length of the biphenylene unit ($\text{Si-C}_{12}\text{H}_8\text{-Si}$), indicating that the units are intercalated perpendicular to the silicate layers. On the other hand, the gallery heights are calculated as 1.94 and 0.91 nm for BESB(2)-ilerite and BESB(4)-ilerite, respectively, showing different intercalation from that of BESB(0)-ilerite. The reduced gallery height of BESB(4)-ilerite indicates the intercalation of the biphenylene unit at an angle of less than 90° to the surface. BESB(2)-ilerite exhibits a larger gallery height than the molecular length of the biphenylene unit. It indicates the intercalation of two biphenylene units in a direction perpendicular to the silicate layers, or, in other words, a bilayer arrangement. Moreover, BESB(2)-ilerite also exhibits a small shoulder at $2\theta = 5.03^\circ$ near the main peak. The d -value ($d = 1.76$ nm) almost corresponds to that of BESB(4), suggesting that BESB(2)-ilerite partially contains a monolayer arrangement of the biphenylene unit similar to BESB(0)- and BESB(4)-ilerite.

TN contents were 2.98, 2.61 and 3.57 wt% for BESB(0)-, BESB(2)- and BESB(4)-ilerite, respectively, before HCl-ethanol or HCl aqueous solution treatment, respectively. After the treatment, the values decreased to less than 0.1 wt% due to the elution of n -hexylamine. TC contents were 19.3, 26.4, and 14.4 wt% for BESB(0)-, BESB(2)- and BESB(4)-ilerite, respectively, after the treatment. It originates from the biphenylene units, indicating their successful immobilization in H-ilerite. We evaluated the number of biphenylene units in a unit cell of H-ilerite from the TC and Si contents. The numbers were 4.2, 5.8 and 2.0 for BESB(0)-, BESB(2)-, and BESB(4)-ilerite, respectively. The numbers increase in the order: BESB(4)- < BESB(0)- < BESB(2)-ilerite. The order corresponds to that of their basal spacings, supporting the notion that the biphenylene units are loaded in the interlayer as a result of the intercalation.

TG curves for BESB(0)-, BESB(2)-, and BESB(4)-ilerite are presented in Fig. 2(a). The TG curves show a weight loss up to

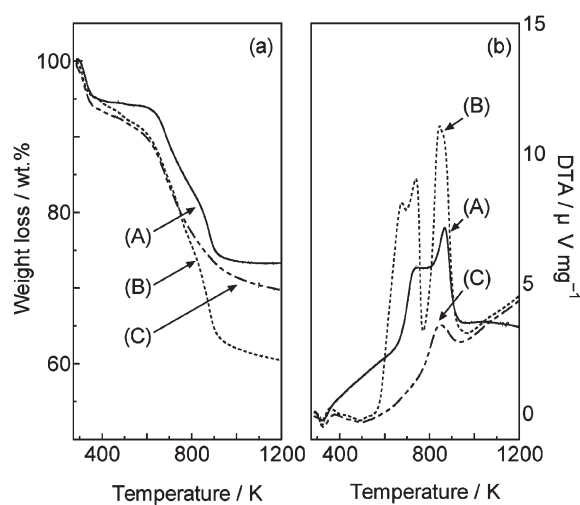


Fig. 2 (a) TG curves of (A) BESB(0)-ilerite, (B) BESB(2)-ilerite, and (C) BESB(4)-ilerite. (b) The corresponding DTA curves of (A) BESB(0)-ilerite, (B) BESB(2)-ilerite, and (C) BESB(4)-ilerite.

423 K due to desorption of water molecules. The curves also show a small loss ranging from 423 to 600 K, which is caused by the dehydration of the silanol groups. The loss is estimated as 0.8, 3.6, and 3.2 wt% for BESB(0)-, BESB(2)-, and BESB(4)-ilerite, respectively. This indicates that BESB(2)- and BESB(4)-ilerite possess more residual silanol groups that are present in H-ilerite and in hydrolyzed BESB molecules. In addition, a large weight loss is observed in the TG curves ranging from 600 to 950 K. Because the losses correspond to TC contents in the products, they are ascribed to the decomposition and full oxidation of the biphenylene unit. The corresponding DTA curves show an exothermic peak around 850 K (Fig. 2(b)). The curves also show another exothermic peak at a temperature lower than 850 K. The products exhibit different peak behaviors: BESB(2)-ilerite (curve B) has two sharp peaks at 673 and 740 K, although BESB(4)-ilerite (curve C) has no peak in the range of 673–740 K. The behaviors probably reflect the structural differences between the products. XRD analyses reveal that BESB(2)-ilerite has the largest d -value of 2.68 nm among the products. The large expansion of the interlayer space might expose the intercalated biphenylene units to the external environment, leading to easy decomposition of the biphenylene unit at a relatively low temperature.

^{29}Si solid-state NMR spectra of H-ilerite and the products are presented in Fig. 3. H-ilerite shows two peaks at -99.7 and -111.9 ppm (curve A). They represent Q^3 ($(\text{SiO})_3\text{SiOH}$) and Q^4 ($(\text{SiO})_4\text{Si}$) structural units that constitute the framework of the silicate sheet in H-ilerite. These peaks are still present in the spectra of the products, although the intensities are changed. The integral ratio (Q^3/Q^4) of H-ilerite is estimated as 1, which is in agreement with the chemical formula reported by Gies *et al.*²⁴ The ratios of the products are summarized in Table 1. They show lower values than that of H-ilerite, indicating that the Q^3 units change to Q^4 units as a result of

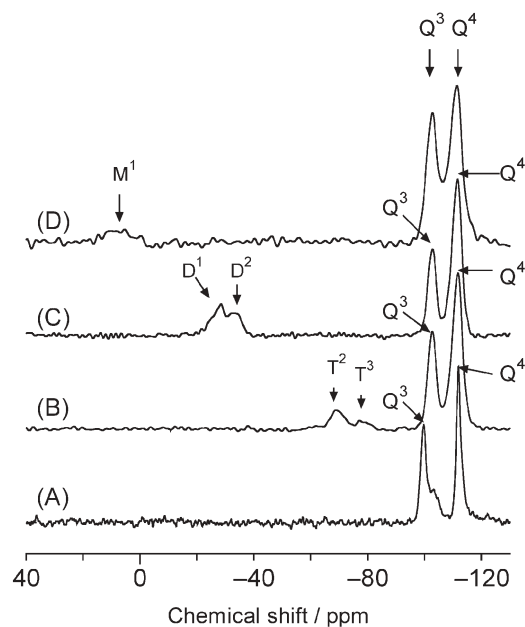


Fig. 3 ^{29}Si solid-state NMR spectra of H-ilerite and biphenylene-bridged ilerites: (A) H-ilerite, (B) BESB(0)-ilerite, (C) BESB(2)-ilerite, and (D) BESB(4)-ilerite.

Table 1 Relative Q^3 and Q^4 intensities of H-ilerite and the products, the number of siloxane bonds generated in the unit cell of H-ilerite and the number of siloxane bonds generated between a biphenylene unit and H-ilerite

	Q^3	Q^4	Q^3/Q^4 ^a	Generated siloxane bonds (N_s)	Generated siloxane bonds between a biphenylene unit and H-ilerite ^b
BESB(0)-ilerite	0.66	1.34	0.49	5.4	1.3
BESB(2)-ilerite	0.61	1.39	0.44	6.2	1.1
BESB(4)-ilerite	0.82	1.18	0.69	2.9	1.5

^a Relative intensities were normalized by the total Q^3 and Q^4 area of H-ilerite. The total area is assumed to be 2.00. ^b The number was calculated as the division of N_s by the number of biphenylene units in the unit cell.

condensation with silanol groups. In addition, BESB(0)-ilerite exhibits two new peaks appearing at -68.8 and -77.3 ppm (curve B). They represent T^2 and T^3 structural units originating from the BESB(0) molecules. The appearance of the T units results from the hydrolysis/condensation of ethoxy groups combined with two silicon atoms on each end of the biphenylene unit. The condensation indicates that the biphenylene units are connected with the silanol groups on the surface of H-ilerite, explaining the decrease of the Q^3 silanol sites. BESB(2)- and BESB(4)-ilerite show similar peaks at -28.5 and -33.2 ppm for BESB(2)-ilerite (curve C), and around 8 ppm for BESB(4)-ilerite (curve D), respectively. They represent D^1 and D^2 structural units for BESB(2)-ilerite, and M^1 for BESB(4)-ilerite, respectively. They also reveal condensation with H-ilerite.

We estimated the number of siloxane bonds generated between the biphenylene unit and the layered framework of H-ilerite from the chemical analyses and the Q^3/Q^4 ratios. The number of siloxane bonds generated in the unit cell of H-ilerite can be calculated as follows:

$$N_s = (1 - Q^3/Q^4)/(1 + Q^3/Q^4) \times N_{sh} \quad (1)$$

where N_s represents the number of siloxane bonds generated in the unit cell, and N_{sh} represents the number of siloxane bonds in H-ilerite. Based on the crystal structure of ilerite, N_{sh} is 16. Q^3/Q^4 represents the integral ratio of the Q^3 peak to the Q^4 peaks for BESB(0)-, BESB(2)-, and BESB(4)-ilerite. The resultant $(1 - Q^3/Q^4)/(1 + Q^3/Q^4)$ leads to the conversion ratio from the silanol group to siloxane bonds after condensation. The N_s values are shown in Table 1. Thus, the number of siloxane bonds generated between a biphenylene unit and H-ilerite is derived from the division of the N_s values by the number of biphenylene units in the unit cell. The numbers for the products are also shown in Table 1. The number (= 1.5) for BESB(4)-ilerite indicates that two ethoxy groups in the BESB(4) molecule are almost completely condensed with H-ilerite. However, the numbers for BESB(0)- and BESB(2)-ilerite are considerably smaller than the numbers of ethoxy groups in these molecules, although they possess 6 and 4 ethoxy groups for BESB(0)- and BESB(2) molecules, respectively. It indicates that 5 or 3 ethoxy groups in the molecules are not condensed with H-ilerite. The NMR spectra of the products suggest that these ethoxy groups are consumed to form condensation with BESB(0) or BESB(2) molecules in the interlayer. As stated above, BESB(0)-ilerite has T^2 and T^3 structural units on the spectra. The units reveal the presence of at least 4 siloxane bonds in one BESB(0)

molecule. In other words, these units reflect 2 or 3 siloxane bonds on the Si atoms bonded to each end of the biphenylene unit, whereas one BESB(0) molecule connects with only one silanol group of H-ilerite. The large numbers of siloxane bonds suggest the condensation with BESB(0)s using the free ethoxy groups. The D^1 and D^2 structural units of BESB(2)-ilerite also indicate condensation with BESB(2)s in the interlayer. As a result, BESB molecules are condensed with H-ilerite, accompanied by considerable condensation with each other in BESB(0) and BESB(2)-ilerite.

3.2. Structural behaviors and the interlayer structure of BESB-ilerites

We investigated *via* the XRD patterns the time dependence of the products in order to examine the stability of the interlayer structures resulting from the condensation of the BESB molecules. XRD patterns of BESB(0)-ilerite with a time-course are presented in Fig. 4(a). The patterns are still retained after the reaction for 499 days, indicating that the structure of BESB(0)-ilerite does not collapse. On the other hand, the peak at $2\theta = 4.56^\circ$ (pattern A), corresponding to the basal spacing, shifts to slightly higher 2θ values with time. The time

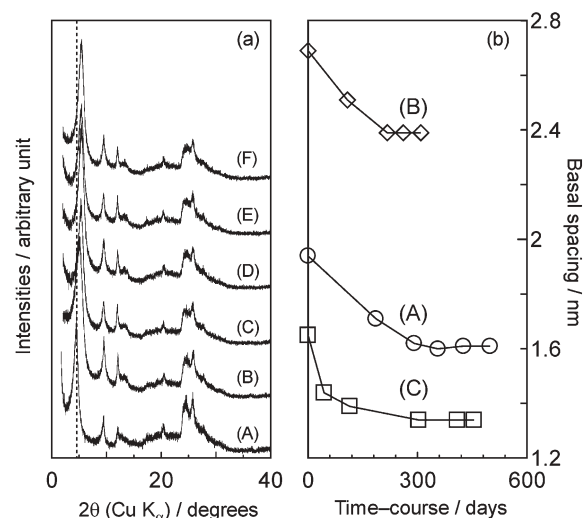


Fig. 4 (a) XRD patterns of BESB(0)-ilerite: (A) after the synthesis, (B) 186 days after the synthesis, (C) 291 days, (D) 356 days, (E) 426 days, and (F) 499 days. The dotted line represents the position of the basal spacing ($2\theta = 4.56^\circ$) of BESB(0)-ilerite before the shift to the higher side of 2θ . (b) Time courses of basal spacings of biphenylene-bridged ilerites: (A) BESB(0)-ilerite, (B) BESB(2)-ilerite, and (C) BESB(4)-ilerite.

dependence of the d -values is shown in Fig. 4(b). The basal spacing of BESB(0)-illerite decreases from 1.94 nm to 1.61 nm up to 356 days (curve A). The decrease in the basal spacings indicates that the interlayer space shrinks along the direction of the stacking of the silicate layers. The shrinkage without destruction suggests that the biphenylene units cause the structural change in the interlayer, maybe changing their sloping orientation relative to the surface. This may be induced by insufficient mechanical stability of the biphenylene units due to poor connection between the biphenylene units and H-illerite, as shown in the NMR results. BESB(2)- and BESB(4)-illerite also show similar behavior without change of the XRD pattern. Their time dependences in Fig. 4(b) show a decrease from 1.65 nm to 1.34 nm for BESB(4)-illerite (curve C) and a decrease from 2.68 nm to 2.39 nm for BESB(2)-illerite (curve B). After decreasing up to around 300 days, the basal spacings become constant at 1.61, 2.39 and 1.34 nm for BESB(0)-, BESB(2)- and BESB(4)-illerite, respectively. As a result, the structures of the products attain stability after the shrinkage of the interlayer spaces.

Diffuse reflective UV-vis absorption spectra are presented for BESB(0)-, BESB(2)-, and BESB(4)-illerite in Fig. 5(a). The samples were measured after the shrinkage of the interlayer space. The spectrum of polymerized BESB(0) is also plotted for comparison. Polymerized BESB(0) shows two peaks at 260 and 280 nm due to absorption from the biphenyl unit (curve A). Similar peaks are observed in the spectra of BESB(0)-, BESB(2)-, and BESB(4)-illerite (curves B–D), indicating the presence of the biphenyl unit in these products. Fluorescence spectra are presented for BESB(0)-, BESB(2)-, BESB(4)-illerite, and polymerized BESB(0) in Fig. 5(b). The peaks are observed at 372, 355, and 330 nm for BESB(0)-, BESB(2)-, and BESB(4)-illerite, respectively (curves B–D), which are caused by fluorescence emission from the biphenylene unit. The peak shifts to longer wavelength in the order:

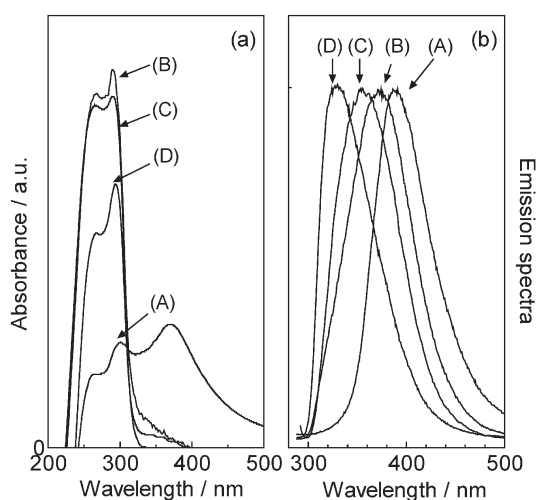


Fig. 5 (a) UV-vis diffuse reflectance spectra of biphenylene-bridged illerites and polymerized BESB(0): (A) polymerized BESB(0), (B) BESB(0)-illerite, (C) BESB(4)-illerite, and (D) BESB(2)-illerite. (b) Fluorescence emission spectra of biphenylene-bridged illerites with polymerized BESB(0): (A) polymerized BESB(0), (B) BESB(0)-illerite, (C) BESB(2)-illerite, and (D) BESB(4)-illerite.

BESB(4) < BESB(2) < BESB(0). Polymerized BESB(0) also shows a peak at 390 nm that exists at a longer wavelength than the others (curve A). Goldenberg *et al.* reported that emission from the biphenyl monomer is observed at 319 nm, the emission showing a red-shift to the higher wavelength side, resulting from the formation of the excimer emission.²⁵ The red-shift at 350–365 nm has also been observed in biphenyl molecules on some clay minerals where the molecules form aggregates on the surface.²⁶ In addition, the conformational transition of bis(4-biphenylmethyl) ether revealed that the excimer emission, originating from the biphenyl dimer, brings about a red-shift to 380 nm.²⁵ These reports indicate that the red-shift from the monomeric emission is inversely correlated with the distance between the neighboring biphenylene units. In other words, the smaller the distance between the biphenylene units, the longer the red-shift. This emission behavior provides information on the molecular arrangement of the biphenylene units in the interlayer. The emission wavelength of BESB(4)-illerite is close to the monomeric emission. This indicates that the biphenylene units are not interacting with each other but are isolated in the interlayer. On the other hand, BESB(0)-illerite exhibits emission at a wavelength similar to that from the dimer, demonstrating that the biphenylene units are close to each other. Polymerized BESB(0), having an emission wavelength near BESB(0)-illerite, supports the notion of a close relation between the neighboring biphenylene units in the interlayer, because polymerized BESB(0) consists of closely packed biphenylene units resulting from the direct connections between the biphenylene units. The emission of BESB(2)-illerite shows at an intermediate wavelength between the monomeric and dimer emissions, indicating that the biphenylene unit exists at an intermediate distance from its neighbors in the interlayer.

3-3. Porosity and surface property of BESB-illerites

Nitrogen adsorption and desorption isotherms before the shrinkage of the interlayer distance showed type-I isotherms of BDDT classification for BESB(0)-, BESB(2)-, and BESB(4)-illerite, respectively.²⁷ These BET surface areas are shown in Table 2. The pore widths, which are derived from the division of the N₂ adsorption uptake around $p/p_0 = 0.9$ by the BET surface area, were estimated as 0.93, 0.91, and 1.00 nm for BESB(0)-, BESB(2)-, and BESB(4)-illerite, respectively. The widths differ from the corresponding gallery heights (estimated from the obtained d -values of the basal plane), being 1.20, 1.94 and 0.91 nm for BESB(0)-, BESB(2)-, and BESB(4)-illerite, respectively. This indicates that the widths reflect not the interlayer distance but the interval between the biphenylene units in the interlayer, assuming that the biphenylene units are present at several Å intervals in the interlayer.

Table 2 Comparison of BET surface areas of the products before and after the decrease in the basal spacing

	BESB(0)-illerite	BESB(2)-illerite	BESB(4)-illerite
Before	616 m ² g ⁻¹	669 m ² g ⁻¹	241 m ² g ⁻¹
After	508 m ² g ⁻¹	578 m ² g ⁻¹	35 m ² g ⁻¹

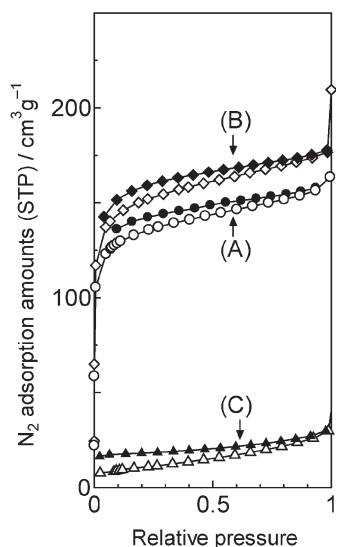


Fig. 6 N_2 adsorption–desorption isotherms of H-ilerite and biphenylene-bridged ilerites after decrease in their basal spacings: (A) BESB(0)-ilerite (\circ : adsorption and \bullet : desorption), (B) BESB(2)-ilerite (\diamond : adsorption and \blacklozenge : desorption) and (C) BESB(4)-ilerite (\triangle : adsorption and \blacktriangle : desorption).

The isotherms after shrinkage are presented for BESB(0)-, BESB(2)-, and BESB(4)-ilerite in Fig. 6. BESB(0)- and BESB(2)-ilerite retain the type-I isotherms that represent microporous materials (curves A and B), although BESB(4)-ilerite has a type-IV isotherm (curve C). This means that only BESB(4)-ilerite changed its isotherm form from type-I to type-IV as a result of shrinkage. Their BET surface areas decreased after shrinkage, as shown in Table 2. The surface area of BESB(4)-ilerite corresponds to that of H-ilerite (BET surface area = $26 \text{ m}^2 \text{ g}^{-1}$), indicating that it is limited to the external surface area. This is caused by the shrinkage of the interlayer space, resulting in the disappearance of vacant spaces. The pore widths are estimated as 0.94 and 0.92 nm for BESB(0)- and BESB(2)-ilerite, respectively. The differences in pore widths before and after shrinkage are less than 0.03 nm, showing that the widths are almost unaffected by shrinkage. In other words, the interval between the biphenylene units is almost constant in spite of the decrease in the interlayer distance. This suggests that the arrangement of the biphenylene units in the interlayer is not destroyed by the shrinkage.

Toluene adsorption isotherms are given for BESB(0)-, BESB(2)-, BESB(4)-ilerite, and H-ilerite in Fig. 7(a). BESB(0)- and BESB(2)-ilerite (curves B and C) exhibit extensively higher toluene uptakes than does H-ilerite (curve A), indicating enhanced adsorptivity for toluene. This is due to the formation of hydrophobic micropores whose framework consists of biphenylene units. Interestingly, BESB(2)-ilerite shows a lower uptake than BESB(0)-ilerite below $P/P_0 < 0.5$. This fact indicates that the surface modification of BESB(2)-ilerite is inferior to that of BESB(0)-ilerite. The lesser modification is probably due to the incomplete condensation of BESB(2) molecules in the interlayer. This results in residual hydrophilic silanols at the ends of biphenylene units disturbing the hydrophobic surface. The toluene isotherm of BESB(0)-ilerite was subsequently compared with those of

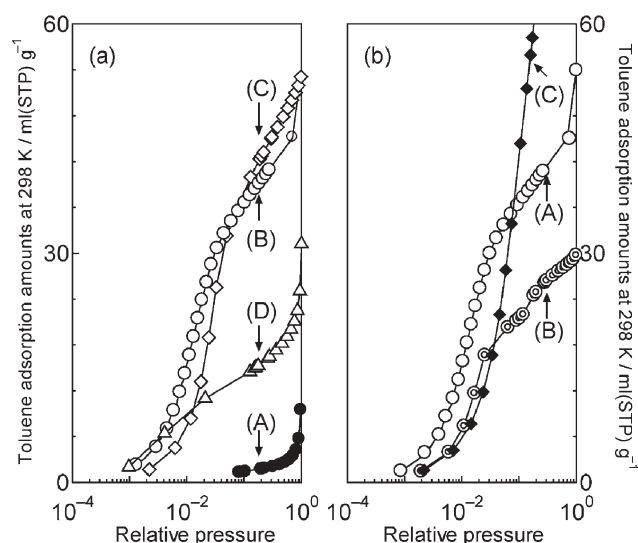


Fig. 7 (a) Toluene adsorption isotherms of H-ilerite and biphenylene-bridged ilerites after decrease in their basal spacings: (A) H-ilerite, (B) BESB(0)-ilerite, (C) BESB(2)-ilerite and (D) BESB(4)-ilerite. (b) A comparison of the toluene adsorption isotherm with those of other silica materials: (A) BESB(0)-ilerite, (B) silicalite, and (C) FSM-22.

hydrophobic silicalite (curve B, BET surface area = $374 \text{ m}^2 \text{ g}^{-1}$) and mesoporous silica (curve C, FSM-22, BET surface area = $958 \text{ m}^2 \text{ g}^{-1}$)²⁸ in Fig. 7(b). BESB(0)-ilerite shows superior adsorptivity below $P/P_0 < 0.5$ to other silica materials. The high adsorptivity will lead to applications as adsorbents, separation devices, and sensor devices for aromatic compounds.

Finally, we investigated the presence of the bridging formation between the silicate layers resulting from the connection between H-ilerite and the biphenylene unit. The adsorption experiment is an appropriate test for evaluating the bridging formation. *p*NA was used as an adsorbate because *p*NA is a nonvolatile aromatic molecule that has high affinity for the micropores of BESB-ilerites. We also used BESB(0)-, BESB(2)-, and BESB(4)-ilerite after synthesizing for 499, 261 and 455 days, respectively, together with CTA-ilerite as an adsorption reference. XRD patterns before and after the adsorption of *p*NA are presented in Fig. 8. CTA-ilerite shows a basal spacing of 2.71 nm (Fig. 8(a), dotted curve). The adsorption of *p*NA enhances the basal spacing to *ca.* 4.0 nm (Fig. 8(a), solid curve), which is estimated as further expansion by 1.3 nm of the interlayer space. The large expansion is caused by the swelling of *p*NA in the interlayer because CTA-ilerite possesses a flexible interlayer space free of volumetric constraint between the layers. The same *p*NA treatments caused a slight increase of the basal spacing from 1.61 to 1.68 nm for BESB(0)-ilerite (Fig. 8(b)), and from 1.34 to 1.37 nm for BESB(4)-ilerite (Fig. 8(d)), respectively. The expansion is estimated as 0.07 and 0.03 nm for BESB(0)- and BESB(4)-ilerite, respectively, and smaller than that of CTA-ilerite. The limited expansion indicates that the biphenylene unit is connected with both surfaces of the silicate layers of H-ilerite, preventing the swelling of *p*NA. Thus, it indicates that the biphenylene units in BESB(0)- and BESB(4)-ilerite make a bridging formation between the layers. On the other

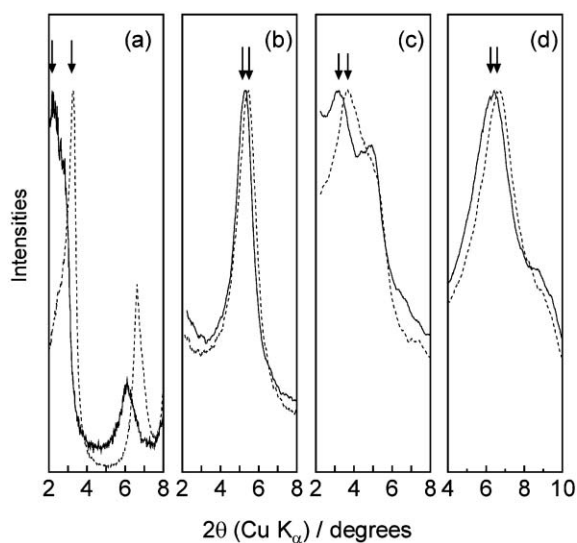


Fig. 8 XRD patterns of biphenylene-bridged ilerites and CTA-ilerite before and after *p*NA treatment: (a) CTA-ilerite (dotted line: before and solid line: after), (b) BESB(0)-ilerite (dotted: before and solid: after), (c) BESB(2)-ilerite (dotted: before and solid: after) and (d) BESB(4)-ilerite (dotted: before and solid: after). The data were smoothed by the Savitzky–Golay method.

hand, BESB(2)-ilerite shows different behavior (Fig. 8(c)). The XRD pattern after adsorption shows a peak at $2\theta = 3.18^\circ$ (solid curve). The peak results from a shift lower than $2\theta = 3.70^\circ$ (dotted curve) of the basal spacing caused by the bilayer arrangement of the biphenylene unit in the interlayer space. The corresponding basal spacing shifts from 2.39 nm to 2.78 nm after the adsorption, calculated as an expansion of 0.39 nm. This expansion is larger than those of BESB(0)- and BESB(4)-ilerite, indicating that the biphenylene units do not completely connect with the consecutive layers. In addition, a new peak is observed at $2\theta = 5.03^\circ$ after the adsorption. This peak corresponds to the shoulder on the main peak before the *p*NA adsorption measurement. It is caused by the monolayer arrangement of the biphenylene unit that is present as a minor phase, indicating connections between the layers similar to those in BESB(0)- and BESB(4)-ilerite. As a result, BESB(2)-ilerite exhibits insufficient bridging formation between the layers.

3-4. Model structures of BESB-ilerites

Structural models of BESB(0)-, BESB(2)-, and BESB(4)-ilerite are given in Fig. 9, based on the discussion above. BESB(0)-ilerite (model (a)) forms an intercalation compound of biphenylene units that bridge the interlayer spaces between the consecutive layers. The bridging formation is achieved by connections between the silanols of H-ilerite and the oligomeric species of the biphenylene units. The oligomeric species consist of condensed biphenylene units such as the dimer in which the phenylene rings are closely parallel to each other. The oligomeric species form vacant spaces between themselves, leading to the creation of slit-shaped micropores that are expected to have high adsorptivity for toluene molecules. The micropores are retained even after the shrinkage caused by

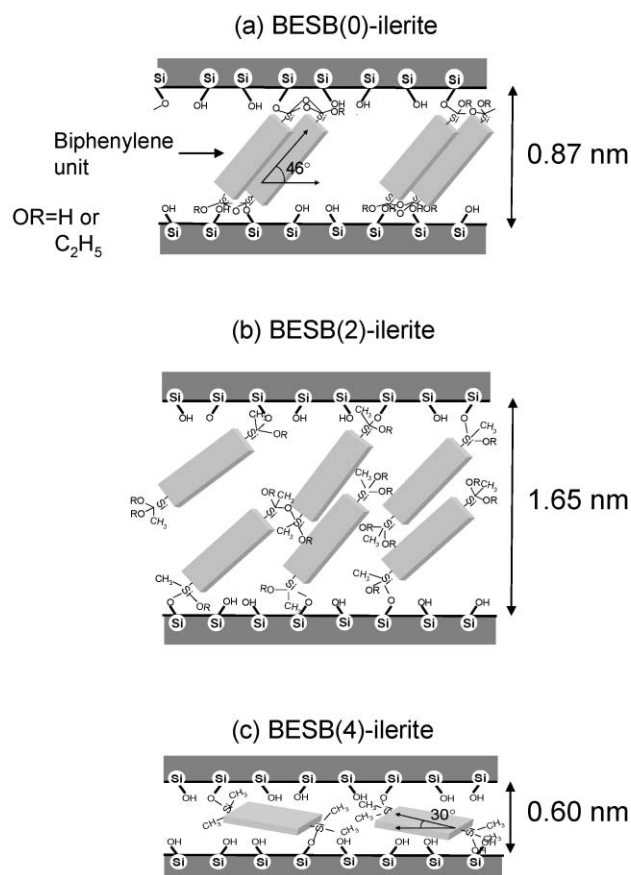


Fig. 9 Model structures of (a) BESB(0)-, (b) BESB(2)-, and (c) BESB(4)-ilerite.

structural change of the oligomeric species in the interlayers. The resultant structure exhibits an open framework containing the oligomeric species in a sloping position at an angle of *ca.* 46° to the silicate surface. BESB(4)-ilerite (model c) also forms an intercalation compound of biphenylene units that are connected with H-ilerite at each end of the biphenylene unit. They are orientated to the silicate layers at an angle of *ca.* 30° , induced by the shrinkage of the interlayer space. The final structure reveals that the biphenylene units are isolated from each other, resulting in the observation of the monomeric emission in the fluorescence spectrum. On the other hand, BESB(2)-ilerite (model b) shows a different structure in the interlayer. XRD results suggest that the biphenylene units mainly form a bilayer arrangement in the interlayer space. The *p*NA adsorption reveals that the biphenylene units do not completely connect with each side of the bilayer, resulting in insufficient bridging formation between the layers. The bilayer arrangement, however, possesses micropores in the interlayer because of the presence of vacant spaces between the biphenylene units. The resultant interlayer structure of BESB(2)-ilerite exhibits an open framework with a flexible interlayer space.

The differences in their interlayer structure are caused by the different reactivity in the three BESB molecules. BESB(0) has three reactive ethoxy groups at each end of the biphenylene unit. The ethoxy groups can not only react with silanols of the H-ilerite layers but also promote the polymerization with each

other. The polymerization induces the formation of the oligomeric species in which the biphenylene units are close to each other because BESB(0) molecules are orientated perpendicular to the silicate surface by the assistance with co-intercalated *n*-hexylamines. BESB(2) and BESB(4) molecule, however, do not cause the polymerization similar to that of BESB(0) molecules in the interlayer. It would be due to the presence of methyl groups which control the condensation between these BESB molecules. The BESB(2) molecule has two methyl groups that might have a role to suppress the 'face-to-face' condensation of the biphenylene units, leading to the bilayer-like aggregates in the interlayer. The higher numbers of the methyl group in BESB(4) molecule has a possibility to inhibit the condensation with the neighboring ethoxy group, forming the isolated bridging formation of BESB(4) molecules in the interlayer. Thus, the control of the reactivity suggests the formation of the various microporous interlayer structures, giving a high possibility to construct novel microporous nanocomposites.²⁹

Conclusions

Microporous layered organic-inorganic hybrid nanocomposites were successfully synthesized by the intercalation and condensation of biphenylene-bridged alkoxy silane compounds, having triethoxysilyl, methyldiethoxysilyl, and dimethylethoxysilyl groups at each end of the 4,4'-biphenylene unit (BESB(0), BESB(2), and BESB(4), respectively), in the interlayer with H-ilerite. Their condensations led to bridging formations between the consecutive layers of H-ilerite, each showing a different interlayer structure. BESB(0) and BESB(4) molecules are present in a monolayer arrangement in which BESB(0) molecules form oligomeric species caused by close stacking like the dimer. The species connect between the layers, leading to a rigid, open framework in the interlayer. BESB(2) molecules form a bilayer arrangement together with partial formation of the monolayer arrangement. The arrangement lacks sufficient connections between the layers, resulting in a flexible, open framework. The structural difference is due to the reactivity in the BESB molecules, which modulate the siloxane formation between the BESB molecules in the interlayer. It suggests that the control of the reactivity in the alkoxy silane compounds has a high possibility of conferring the ability to design various organic-inorganic interlayer structures with an open framework. On the other hand, the poor siloxane formation of the BESB molecules with H-ilerite affected the mechanical stability of the biphenylene units as 'pillars' capable of retaining the interlayer space, causing a slight shrinkage of the interlayer space. The resultant BESB(0)- and BESB(2)-ilerite, however, had high microporosity originating from the open framework in the interlayer, showing superior adsorptivity for toluene and a potential for application as adsorbents or in sensor devices. Consequently, this approach

will lead to the construction of novel microporous materials, the key to improved selectivity and activity in separation and catalytic applications.

Acknowledgements

R. I. is grateful to Dr Y. Shinohara (Tsukuba University, Japan) for many helpful discussions.

References

- 1 E. Ruiz-Hitzky and J. M. Rojo, *Nature*, 1980, **287**, 28–30.
- 2 E. Ruiz-Hitzky, J. M. Rojo and G. Lagaly, *Colloid Polym. Sci.*, 1985, **263**, 1025–1030.
- 3 T. Yanagisawa, K. Kuroda and C. Kato, *React. Solids*, 1988, **5**, 167–175.
- 4 T. Yanagisawa, K. Kuroda and C. Kato, *Bull. Chem. Soc. Jpn.*, 1988, **61**, 3743–3745.
- 5 T. Yanagisawa, M. Harayama, K. Kuroda and C. Kato, *Solid State Ionics*, 1990, **42**, 15–19.
- 6 M. Ogawa, S. Okutomo and K. Kuroda, *J. Am. Chem. Soc.*, 1998, **120**, 7361–7362.
- 7 S. Okutomo, K. Kuroda and M. Ogawa, *Appl. Clay Sci.*, 1999, **15**, 253–264.
- 8 K. Isoda, K. Kuroda and M. Ogawa, *Chem. Mater.*, 2000, **12**, 1702–1707.
- 9 M. Ogawa, M. Miyoshi and K. Kuroda, *Chem. Mater.*, 1998, **10**, 3787–3789.
- 10 T. Ikeda, Y. Akiyama, Y. Oumi, A. Kawai and F. Mizukami, *Angew. Chem., Int. Ed.*, 2004, **43**, 4892–4896.
- 11 R. Millini, L. C. Carluccio, A. Carati, G. Bellussi, C. Perego, G. Cruciani and S. Zanardi, *Microporous Mesoporous Mater.*, 2004, **74**, 59–71.
- 12 S. Zanardi, A. Alberti, G. Cruciani, A. Corma, V. Fornés and M. Brunelli, *Angew. Chem., Int. Ed.*, 2004, **43**, 4933–4937.
- 13 Y. X. Wang, H. Gies, B. Marler and U. Muller, *Chem. Mater.*, 2005, **17**, 43–49.
- 14 D. Mochizuki, A. Shimojima, T. Imagawa and K. Kuroda, *J. Am. Chem. Soc.*, 2005, **127**, 7183–7191.
- 15 D. Mochizuki and K. Kuroda, *New J. Chem.*, 2006, **30**, 277–284.
- 16 A. Shimojima, D. Mochizuki and K. Kuroda, *Chem. Mater.*, 2001, **13**, 3603–3609.
- 17 R. Ishii and Y. Shinohara, *J. Mater. Chem.*, 2005, **15**, 551–553.
- 18 K. J. Shea, D. A. Loy and O. Webster, *J. Am. Chem. Soc.*, 1992, **114**, 6700–6710.
- 19 D. A. Loy and K. J. Shea, *Chem. Rev.*, 1995, **95**, 1431.
- 20 B. Boury and R. J. P. Corriu, *Chem. Commun.*, 2002, 795–802.
- 21 B. Boury, F. Ben, R. J. P. Corriu, P. Delord and M. Nobili, *Chem. Mater.*, 2002, **14**, 730–738.
- 22 H. Muramatsu, R. Corriu and R. Boury, *J. Am. Chem. Soc.*, 2003, **125**, 854–855.
- 23 K. Kosuge and A. Tsunashima, *J. Chem. Soc., Chem. Commun.*, 1995, 2427–2428.
- 24 S. Vortmann, J. Rius, S. Siegmann and H. Gies, *J. Phys. Chem. B*, 1997, **101**, 1292–1297.
- 25 M. Goldenberg, J. Emert and H. Morawetz, *J. Am. Chem. Soc.*, 1978, **100**, 7171–7177.
- 26 A. P. P. Cione, J. C. Scaiano, M. G. Neumann and F. Gessner, *J. Photochem. Photobiol., A*, 1998, **118**, 205–209.
- 27 S. J. Gregg and K. S. W. Sing, *Adsorption, Surface Area and Porosity 2nd Edn.*, Academic Press, London, 1982, p. 3.
- 28 S. Inagaki, Y. Fukushima and K. Kuroda, *J. Chem. Soc., Chem. Commun.*, 1993, 680–682.
- 29 S. Komarneni, *J. Mater. Chem.*, 1992, **2**, 1219–1230.